



HAL
open science

Description of the variation of retention versus pH in nanofiltration of organic acids

Yin Zhu, Sylvain Galier, H el ene Roux-de Balmann

► To cite this version:

Yin Zhu, Sylvain Galier, H el ene Roux-de Balmann. Description of the variation of retention versus pH in nanofiltration of organic acids. *Journal of Membrane Science*, 2021, 637, pp.119588. 10.1016/j.memsci.2021.119588 . hal-03339748

HAL Id: hal-03339748

<https://hal.science/hal-03339748>

Submitted on 9 Sep 2021

HAL is a multi-disciplinary open access archive for the deposit and dissemination of scientific research documents, whether they are published or not. The documents may come from teaching and research institutions in France or abroad, or from public or private research centers.

L'archive ouverte pluridisciplinaire **HAL**, est destin ee au d ep ot et  a la diffusion de documents scientifiques de niveau recherche, publi es ou non,  emanant des  tablissements d'enseignement et de recherche fran ais ou  trangers, des laboratoires publics ou priv es.



[Open Archive Toulouse Archive Ouverte](https://oatao.univ-toulouse.fr/)

OATAO is an open access repository that collects the work of Toulouse researchers and makes it freely available over the web where possible

This is an author's version published in: <http://oatao.univ-toulouse.fr/28256>

Official URL : <https://doi.org/10.1016/j.memsci.2021.119588>

To cite this version:

Zhu, Yin^{ORCID} and Galier, Sylvain^{ORCID} and Roux-de Balmann, H el ene^{ORCID}
Description of the variation of retention versus pH in nanofiltration of organic acids. (2021) Journal of Membrane Science, 637. ISSN 0376-7388

Any correspondence concerning this service should be sent
to the repository administrator: tech-oatao@listes-diff.inp-toulouse.fr

Description of the variation of retention versus pH in nanofiltration of organic acids

Yin Zhu, Sylvain Galier, H el ene Roux-de Balmann*

Laboratoire de G enie Chimique, Universit e de Toulouse, CNRS, INPT, UPS, Toulouse, France

ARTICLE INFO

Keywords:

Biomass valorization
Volatile fatty acids
Membrane processes
Nanofiltration
Retention

ABSTRACT

Nanofiltration can be used to recover chemicals, like VFAs, produced by the fermentation of biomass. Solution pH is a key parameter for fermentation as well as for recovery using nanofiltration. Current work reports an experimental investigation carried out with single and mixed solutions that contain acetic, propionic, and butyric acids, at various concentrations and pHs. It is shown that retention of VFAs increases with solution pH following an S-shaped curve related to the VFA dissociation. Retentions of VFAs decrease with the concentration, the influence being negligible at low pH values and more significant at high pH values. A simple model is proposed to calculate VFAs retentions versus pH for different concentrations and a given filtration flux, considering the dissociation of VFAs and the retention of dissociated and undissociated solutes. Calculated retentions can fit well with the experimental ones, on condition to consider solutes pK_a values slightly higher than theoretical ones, up to 1.24 pH units, or a variation of the membrane charge with pH, corresponding to an effective membrane pK_a between 5.44 and 5.80. Both assumptions are supported by previous investigations.

1. Introduction

Volatile fatty acids (VFAs), also referred to as short-chain fatty acids (SCFAs), are carboxylic acids with less than six carbon atoms [1]. Nowadays, VFAs are considered as one type of promising chemical building blocks in the biorefinery concept [2]. Acetic (Ac), propionic (Pr), and butyric (Bu) acids are the main products in VFAs fermentation broth. Membrane process, e.g., nanofiltration (NF), can be considered for the separation and purification of VFAs from fermentation broth [2]. The few reports dealing with the nanofiltration of VFAs have shown that the recovery and purification of VFAs by NF are strongly influenced by solution pH [3–5]. It was also reported that the fermentation is strongly influenced by the pH, which fixes the productivity and the composition of VFAs obtained [6].

Thin-film composite membranes (TFCM), like NF-45 used in this work, are composed of a thin nanoporous active layer made of polyamide, with a macroporous supporting layer made of polysulfone [7]. The membrane charge can come from the dissociation of functional groups and adsorption of ions, polyelectrolytes, ionic surfactants, and charged macromolecules from solution [8]. Dissociation of functional groups (carboxylic and amino groups) on the active layer is commonly considered as the main contribution of the pH-dependent membrane

charge [9–11]. When the solution pH is higher than the membrane isoelectric point (IEP), the membrane surface charge increases with pH and reaches a plateau value at pH of about 7–8. This was demonstrated by the measurement of the membrane zeta potential [12,13], as well as by mathematical modeling [14]. Thus, an effective pK_a value can be estimated for the membrane, that is, the average pK_a value of all the functional groups. Contact angle titration was used to determine the effective pK_a values of various polyamide films, and values from 5 to 9 were obtained for different solutions [15]. Recently, heavy ions probes were used to determine the membrane charge. It was suggested that the membrane functional groups have different pK_a values, and then the dissociation curve of membrane functional groups can be fitted considering two pK_a values [9,10].

For the nanofiltration of a neutral solute, the charge interaction between the solute and the membrane is negligible, and the retention is fixed according to size effect. Therefore, the retention of a neutral solute is independent of both concentration and solution pH [16,17]. For the nanofiltration of a charged solute, the retention is fixed by a combination of size and charge effect. However, for a solute, the molecular weight of which is higher than the membrane MWCO, high retention is observed regardless of the solute and membrane charge [18]. In this case, the size effect is the dominating factor, and the influences of both

* Corresponding author.

E-mail address: roux@chimie.ups-tlse.fr (H. Roux-de Balmann).

concentration and pH are negligible [19,20]. On the other hand, when the solute molecular weight is lower than the MWCO of the membrane, both size and charge effects play a significant role, and the retention depends on both the concentration and the pH.

For strong electrolytes, the pH has no impact on the solute charge. The influence of pH on solutes retention is then due to the dissociation of membrane functional groups that fixes the membrane charge. For small symmetric salts, e.g., NaCl and KCl, it was shown that when the solution pH becomes higher than the IEP of the membrane, the retentions of salts increase with pH due to the increase of membrane charge [12,17,21,22].

However, for the nanofiltration of weak electrolytes such as organic acids, the retention mechanism is more complex, as both the membrane and solute charge vary with the solution pH [23,24]. For a small monovalent organic acid, i.e., acetic acid, with an MW (60 g mol^{-1}) much lower than the MWCO of the nanofiltration membrane (200–500 g mol^{-1}), low retention is expected at low pH since it is uncharged. When the pH increases, the proportion of dissociated acetic acid (acetate that is anionic) increases; meanwhile, the membrane surface charge also increases. The electrostatic interactions between membrane and solutes are then stronger, and higher retention is observed. Then the retention of weak acids is expected to increase with solution pH following an S-shaped dissociation curve. Indeed, it was reported that the retention of acetic acid increases from nearly 0% at pH 2.9 (neutral) to more than 90% at pH 9.1 (dissociated) following an S-shaped curve [25–27]. This S-shaped retention curve was also observed during nanofiltration of sulfamethoxazole and ibuprofen by a loose NF membrane [28], as well as nanofiltration of succinic acid [29] and sulfuric acid [30–32]. However, this effect of pH is less pronounced at higher concentrations because of the screening effect [17].

On the other hand, it was suggested that for a weak electrolyte like organic acids, the solute flux could be estimated according to the dissociation of the solute [33–35]. As a result, the retention is given as the weighted average of the retentions of undissociated and dissociated forms, the proportions of which are determined from the solute pK_a and solution pH. For NF of lactic acid, it was shown that the mass transfer parameter of undissociated lactic acid is independent of the solution pH, while the mass transfer parameter of dissociated lactic acid (lactate) linearly increases with pH. It was further concluded that the retention of lactic acid at different pH could be simulated using these two parameters [34]. However, in this study, only a short range of pH values (2.88–4.93) was investigated, and the influence of the concentration was not discussed.

Then, the present work aims to investigate the retention of VFAs and especially the influence of the pH and concentration. Single and mixed solutions of different compositions (proportions of VFAs) and total concentrations are used in a range of pH values from 3 to 8. The objective is to check if a simple model can be proposed to describe the variation of the VFA retention versus pH in a wide range of operating conditions.

2. Materials and methods

A flat sheet composite membrane, NF 45 (Filmtec, Dow), was used in this work. The membrane is a composite thin film membrane with polyamide as the active layer and polysulfone/polyester as the support layer, the MWCO is about 200 g mol^{-1} , the IEP of the membrane is about 4, and the pure water permeability is about $1.6 \times 10^{-6} \text{ m s}^{-1} \cdot \text{bar}^{-1}$ at 25°C (Table 1). Different pHs are investigated from 3 to 8. The synthetic

Table 1
Characteristics of NF-45, Dow Filmtec membrane.

MWCO (g. mol^{-1})	Material	Maximum Temperature ($^\circ\text{C}$)	Max. pressure (bar)	pH range	Membrane isoelectric point	Pure water permeability ($\text{m}\cdot\text{s}^{-1}\cdot\text{bar}^{-1}$, 25°C)
200	Polyamide/polysulfone/polyester	45°C	41 [36]	2-12 (recommended 3-10)	4.0 [37]	1.57×10^{-6} [38]

solutions of VFAs at pH 8 were prepared using sodium acetate (NaAc), sodium propionate (NaPr), sodium butyrate (NaBu). Solutions at pH lower than 8 were prepared using acetic (HAc), propionic (HPr), and butyric (HBU) acids dissolved in ultra-pure water, and the pH was adjusted with a solution of NaOH at 2 mol L^{-1} . Table 2 shows the main characteristics of the solutes. The compositions of feed solutions in single, binary, and ternary mixtures are summarized in Table 3. Three total concentrations were investigated (100 mM, 200 mM, and 500 mM).

2.1. Analytical methods

The concentrations of VFAs in single solutions were measured by a refractometer (ATAGO AX500, USA). VFAs concentrations in mixed solutions were obtained by High-Performance Liquid Chromatography (HPLC) (Jasco LC Net II/ADC, Japan) equipped with a Shodex SH1011 (Showa Denko, Japan) column and a UV detector (wavelength was set at 280 nm). The column temperature was set at 50°C , and 10 mM of sulfuric acid was used as the mobile phase at a flow rate of 1 mL min^{-1} . The injection volume was $10 \mu\text{l}$, and the samples were diluted to the concentration range from 5 mM to 50 mM.

2.2. Experimental procedure

NF experiments were carried out using a dead-end stirred filtration cell. The total volume of the cell was 400 mL. The stirring speed was set at 108 rpm. One piece of NF-45 membrane was placed at the bottom of the cell, supported by a stainless steel porous disc. The active surface of the membrane was 30 cm^2 . Pressurized air was used to pressurize the cell as the driven force. The driven pressure was controlled manually by a valve. Filtration was operated at room temperature (between 20 and 27°C). Permeate was timed and measured by an electronic balance to calculate the filtration flux.

Membrane conditioning and cleaning procedures are crucial to obtain accurate data. The membrane was first immersed in ultra-pure water for 24 h. It was then compacted by filtering ultra-pure water at a pressure of 20 bar until the filtration flux, J reaches a constant value. The linearity of J versus ΔP was checked, and the mean hydraulic permeability L_{p0} was calculated by the slope of $J/\Delta P$. After each NF experiment, the membrane was washed twice by filtering 200 mL of ultra-pure water, and pure water permeability was measured to check any membrane fouling or aging.

In addition to pure water permeability, retention of glucose (molecular weight: 180 g mol^{-1}) was used as a reference to detect any membrane modification during the experiments. Once a membrane sample presents visible mechanical damage, an abnormally pure water

Table 2
Characteristics of VFAs.

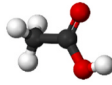
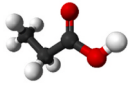
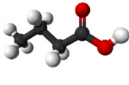
Name	Acetic acid	Propionic acid	Butyric acid
Structure			
Molecular weight (g. mol^{-1})	60.05	74.08	88.11
pK_a (25°C)	4.76	4.88	4.82

Table 3

Proportions of the synthetic solutions for three total concentrations, 100 mM, 200 mM and 500 mM.

Solute	Single solution			Mixed solutions		
	s1	s2	s3	s4	s5	s6
Acetate/Acetic acid	1			1/2	1/2	1/3
Propionate/Propionic acid		1		1/2		1/3
Butyrate/Propionic acid			1		1/2	1/3

permeability (more than 20% difference between two consecutive permeability measurements), or a significant increase or decrease of Glucose rejection (more than 5%), it was replaced by a new one. Three pieces of the membrane were used for all the experiments reported in this work, the pure water permeability values of those membranes for the entire period of time were within the range from $1.6 \times 10^{-6} \text{ m s}^{-1} \text{ bar}^{-1}$ to $2.0 \times 10^{-6} \text{ m s}^{-1} \text{ bar}^{-1}$, and the glucose retentions are between 90% and 93% at a transmembrane pressure of 20 bar.

For each experiment, 400 mL of solution was initially fed into the cell. Then, the pressure was increased step by step (4, 8, 12, 16, 20 bar). For each pressure investigated, the filtration flux was measured after reaching a steady-state, and 1.5–2 mL of permeate was then collected for analysis. For each experiment, approximately 60 mL of permeate was collected in total. It means that in the worst case, the concentration factor would be equal to 1.15. In addition, the feed volume, V_f , permeate volume, V_p , and retentate volume V_r , were determined, as well as the concentrations of the feed C_f , permeate, C_p , and retentate, C_r , using the previously detailed analytical methods. The mass balance, $V_f C_f = V_p C_p + V_r C_r$, was checked, and it was observed that the maximum difference does not exceed 5%.

2.3. Model used to describe the retention versus pH

The filtration flux, J , was calculated by Eq. (1).

$$J = \frac{V_p}{S_m \times t} \quad (1)$$

with the volume of permeate V_p (m^3), obtained by the weight of permeate; S_m the active surface of the NF membrane (m^2) and the unit of time, t in second (s).

The values of solute retention, R , were obtained using the following expression:

$$R = \left(1 - \frac{C_p}{C_f}\right) \times 100 (\%) \quad (2)$$

where C_f is the initial feed concentration and C_p is the permeate concentration.

The retention versus filtration flux curves were fitted using a simple model with two parameters proposed by Timmer et al. [34]:

$$R = \frac{A \times J}{J + B} \quad (3)$$

As mentioned before, during the experiments, 60 mL of permeate was collected, so that the concentration in the retentate increased. Then, the retention calculated using the initial feed concentration is underestimated. However, it was checked that this underestimation does not exceed 3% and does not change the trends that will be discussed.

The total concentrations of VFAs in the feed and permeate are given in Eq. (4) and Eq. (5).

$$C_f^{VFAs} = \sum_{i=1}^n C_f^i \quad (4)$$

$$C_p^{VFAs} = \sum_{i=1}^n C_p^i \quad (5)$$

C_f^i and C_p^i represent the concentration of individual VFA i in the feed and permeate solution, respectively.

Then the global retention of VFAs, representing the total VFAs retention, is defined in Eq. (6).

$$R_{glo}^{VFAs} = 1 - \frac{C_p^{VFAs}}{C_f^{VFAs}} = 1 - \frac{\sum_{i=1}^n C_p^i}{\sum_{i=1}^n C_f^i} \quad (6)$$

Eq. (6) can be rewritten as the weighted average of individual VFAs retentions, considering the proportion of individual solute in the mixed solution,

$$R_{glo}^{VFAs} = \sum_{i=1}^n P^i R_{mix}^i \quad (7)$$

In Eq. (7), R_{mix}^i is the retention of individual VFA i in the mixed solution, P^i the proportion of individual VFA i in the mixed solution, and the sum of the proportions of individual VFA i is equal to 1.

$$\sum_{i=1}^n P^i = 1 \quad (8)$$

The proportion of dissociated VFAs in the single solution is given in Eq. (9).

$$P_{VFAs^-} = \frac{10^{pH-pK_{ai}}}{1 + 10^{pH-pK_{ai}}} \quad (9)$$

where pK_{ai} is the pK_a value of individual VFA i .

For a mixed solution, the total proportion of dissociated VFAs, P_{VFAs^-} , is the sum of the individual proportions, P_i ,

$$P_{VFAs^-} = \sum_{i=1}^n \left(P_i \times \frac{10^{pH-pK_{ai}}}{1 + 10^{pH-pK_{ai}}} \right) \quad (10)$$

The total proportion of dissociated VFAs, P_{VFAs^-} , can also be calculated using an average pK_a , pK_{a-mix} , for the mixed solution, as shown in Eq. (11),

$$P_{VFAs^-} = \frac{10^{pH-pK_{a-mix}}}{1 + 10^{pH-pK_{a-mix}}} \quad (11)$$

pK_{a-mix} is defined as Eq. (12),

$$pK_{a-mix} = \sum_{i=1}^n (P_i \times pK_{ai}) \quad (12)$$

For the pH range investigated, the difference between Eq. (10) and Eq. (11) is below 0.06%. Further calculation requires the pK_a values of single and mixed solutions; then, for easier comparison, Eq. (11) is used to discuss the dissociation of VFAs in mixed solutions.

As previously mentioned, it was reported that the retention of a weak acid, like VFA, is a combination of the retentions of its dissociated and undissociated forms [33–35]. Then the retention of VFAs can be calculated using the following equation, considering the proportions of the two forms.

$$R_{VFAs}^{cal} = R_{HVFAs} \times (1 - P_{VFAs^-}) + R_{VFAs^-} (C_{VFAs^-}) \times P_{VFAs^-} \quad (13)$$

P_{VFAs^-} is the proportion of dissociated VFAs in the solution obtained from Eqs. (9) and (11), R_{HVFAs} is the retention of undissociated VFAs, and $R_{VFAs^-} (C_{VFAs^-})$ is the retention of dissociated VFAs.

Eq. (13) is used with the following assumptions: (1) Retention of HVFAs, R_{HVFAs} is that obtained at pH 3 and does not depend on the concentration, (2) Retention of $VFAs^-$, $R_{VFAs^-} (C_{VFAs^-})$ is that obtained at pH 8 at the corresponding ionic concentration.

The calculation of the second term in Eq. (13) requires knowing the values of the retention of the dissociated VFA, $R_{VFAs^-} (C_{VFAs^-})$, versus the ionic concentration. This is obtained from experimental retentions obtained at pH 8, by fitting the variation of retention versus concentration.

In the following parts, the model mentioned above is used to describe

the retention of VFAs in single and mixed solutions.

3. Results and discussions

Experiments are firstly carried out with single solute solutions, then for binary and ternary mixed solutions containing acetic, propionic, and butyric acids. The influence of operating conditions (pH, pressure, etc.), as well as the total concentration on the retention of VFAs, are investigated. Then, based on the dissociation of both solutes and membrane, Eq. (13) is used to describe the variation of VFAs retention versus pH at a given filtration flux.

3.1. Solutes retention in single and mixed solutions

3.1.1. Single solutions

Retentions of acetate/acetic acid (Ac), propionate/propionic acid (Pr), and butyrate/butyric acid (Bu) at different solution pH and three total concentrations are plotted versus filtration flux in Fig. 1. The curves are fitted according to the model proposed by J. M. K. Timmer et al. [34], and the solute retention at a given filtration flux is calculated from the fitted equation Eq. (3). Retentions at $J_1 = 0.2 \times 10^{-5} \text{ m s}^{-1}$, $J_2 = 0.5 \times 10^{-5} \text{ m s}^{-1}$, $J_3 = 1 \times 10^{-5} \text{ m s}^{-1}$, and $J_4 = 1.5 \times 10^{-5} \text{ m s}^{-1}$ are obtained from the fitting curves for different concentrations. For 500 mM, only J_1 is shown since the other filtration flux values are not in the

experimental range.

For any condition, one can observe that the retention of VFAs increase with the filtration flux. Then, at given filtration flux, the retention of the three VFAs increase when the solution pH increases. The lowest retentions of Ac and Pr are observed at pH 3. The experimental results of the retention of Bu at pH 3 are not obtained. The VFAs retention at pH 3 seems not influenced by concentration. Retentions of Ac at 100 mM and 500 mM are similar, i.e., 2% at the filtration flux of J_3 . For propionate as well, retentions are similar for the two concentrations (100 mM and 500 mM) and about 4% at the filtration flux of J_3 . The highest retentions are observed at pH 8 for the three VFAs. Moreover, the retention at high pH is more concentration-dependent. It is observed that the retention of VFAs decreases when the concentration increases. For instance, the retentions of Ac at three concentrations (100 mM, 200 mM, and 500 mM) are 65%, 59%, and 38% respectively for a filtration flux of J_1 ($0.2 \times 10^{-5} \text{ m s}^{-1}$) at pH 8.

As indicated in the introduction, the retention mechanism of VFAs by NF membrane is a combination of size and charge effect. At pH 3, VFAs are uncharged, and the retention is mainly due to size effect. Since VFAs have much lower MWs than the MWCO of the membrane, low retention is expected. Besides, it is known that the influence of concentration on the retention of a neutral solute is negligible, as reported for glucose solutions, for instance, both in single [16,39] and mixed (glucose/x-ylose) solutions [40]. Then the concentration is expected to have a

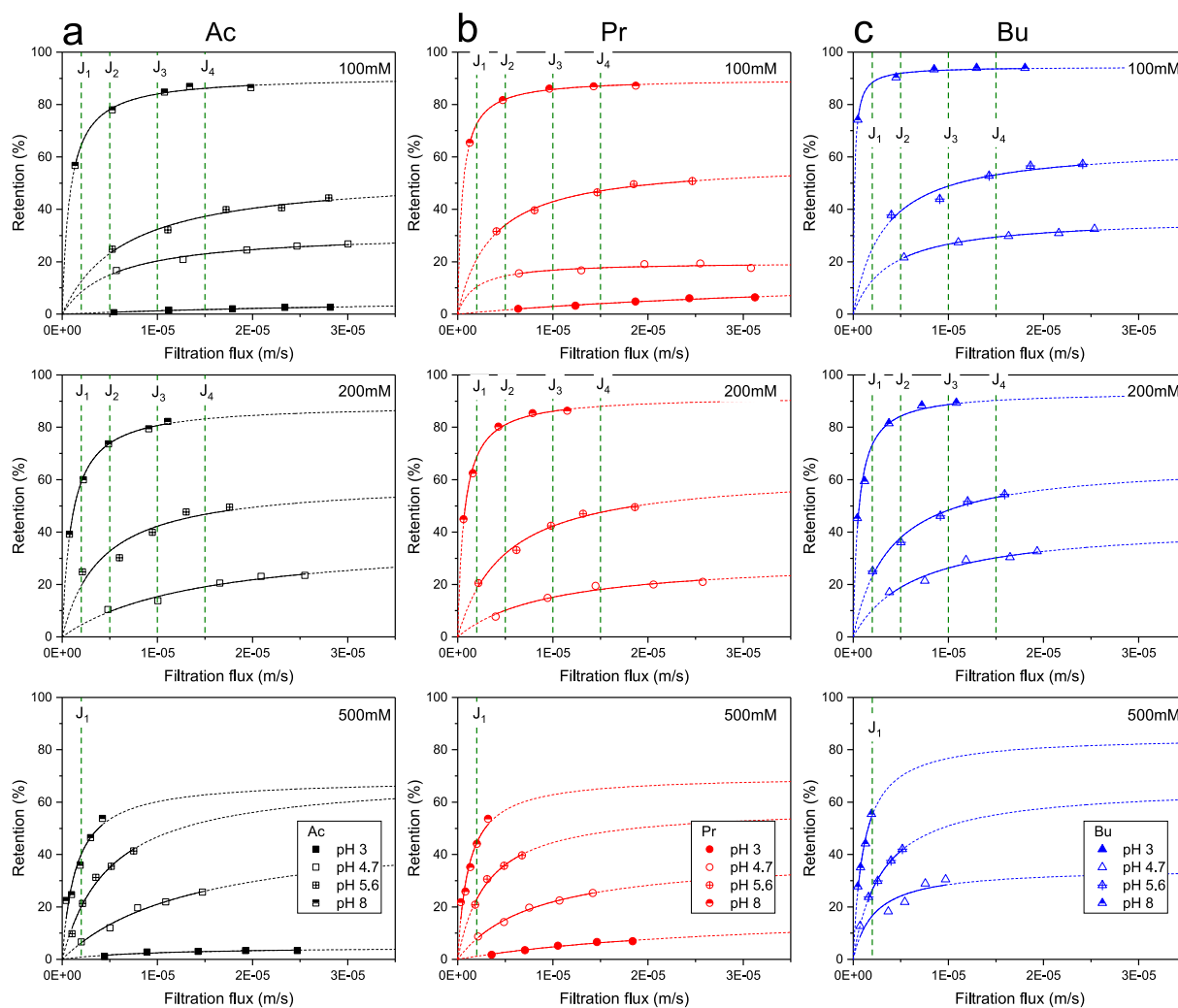


Fig. 1. Retentions of VFAs single solutions versus filtration flux at different solution pH and varying total concentration, (a) Ac, (b) Pr, (c) Bu. The fitting curves are obtained from the model proposed in Ref. [34]. Retentions at $J_1 = 0.2 \times 10^{-5} \text{ m s}^{-1}$, $J_2 = 0.5 \times 10^{-5} \text{ m s}^{-1}$, $J_3 = 1 \times 10^{-5} \text{ m s}^{-1}$, and $J_4 = 1.5 \times 10^{-5} \text{ m s}^{-1}$ are compared, for 500 mM, only J_1 is in the experimental range.

negligible influence on the retention of VFAs at pH 3, as observed.

On the contrary, at pH 8, both the VFAs and the membrane are charged, and the charge effect plays an essential role in VFAs retention. Indeed, much higher retentions than those obtained at pH 3 are observed, and the retentions increase with solution pH from 3 to 8. Similar results were also reported in previous works investigating the retention of weak acids [25,29–31]. Furthermore, when the concentration of VFAs increases, the ionic strength of the solution increases, and then the charge interactions between membrane and VFAs are weakened. This is reported as a screening effect [29,39], according to which the retention is expected to decrease with the concentration, as observed.

The retentions of Ac, Pr, and Bu at given filtration flux ($J_1, J_2, J_3,$ and J_4) versus solution pH for the three concentrations are plotted in Fig. 2. The fitting curves of solutes retentions versus pH are obtained from sigmoid curve fitting by Origin®. The dissociation curves of Ac, Pr, and Bu, obtained from Eq. (9), are also plotted as references. For the concentration of 500 mM, the filtration flux is much lower than that at lower concentrations, then only the retentions at J_1 are shown.

One can observe that the increase of the individual VFA retentions versus the solution pH follows a sigmoid curve for any filtration flux investigated. For a given pH, the retention increases for increasing filtration flux. Moreover, retention follows the dissociation curve.

These results agree with previous ones obtained with other weak acids, like succinic acid. It was reported that, for different filtration flux, the retention increases with the solution pH following the fraction of the divalent form (Suc^{2-}) [29].

3.1.2. Mixed solutions

The retentions of individual Ac, Pr, and Bu in ternary solutions (Ac: Pr: Bu = 33%: 33%: 33%) at given filtration flux ($J_1, 0.2 \times 10^{-5} \text{ m s}^{-1}$) and three total concentrations (100 mM, 200 mM, and 500 mM) are plotted versus solution pH in Fig. 3a. The retentions of VFAs in single solutions at the same concentration and filtration flux are also given as references. Results obtained for the other three filtration fluxes ($J_2, J_3,$ and J_4) show similar behavior to that observed at J_1 . Those results are thus not shown.

As observed for single solutions, the individual VFAs retentions in mixed solutions increase with pH following an S-shape curve. An exception is found for the retention of Ac at the highest concentration (500 mM) that firstly increases with the pH, reaches a maximum at pH 6.6, and decreases when the pH increases to 8.

At low pH values, the individual VFAs retentions in the mixed solutions are similar to those in single solutions at the same concentration. However, at a high pH value (pH 8), the individual VFAs retentions in single and mixed solutions are different. In the mixed solution, the retention of the most retained VFA, Bu, is similar to that in the single solution. In contrast, the retention of the least retained VFA, Ac, is lower than in the single solution and that of the intermediately retained VFA, Pr, nearly unchanged between single and mixed solutions. Then the retention differences between VFAs in the mixed solutions are more significant compared to those in single solutions, especially at high concentrations. Furthermore, one can observe that the retentions of individual VFAs follow the same sequence (Ac < Pr < Bu) for the three total concentrations and whatever the solution pH between 3 and 8.

Retention of VFAs at low pH is mainly fixed by size effect. The co-

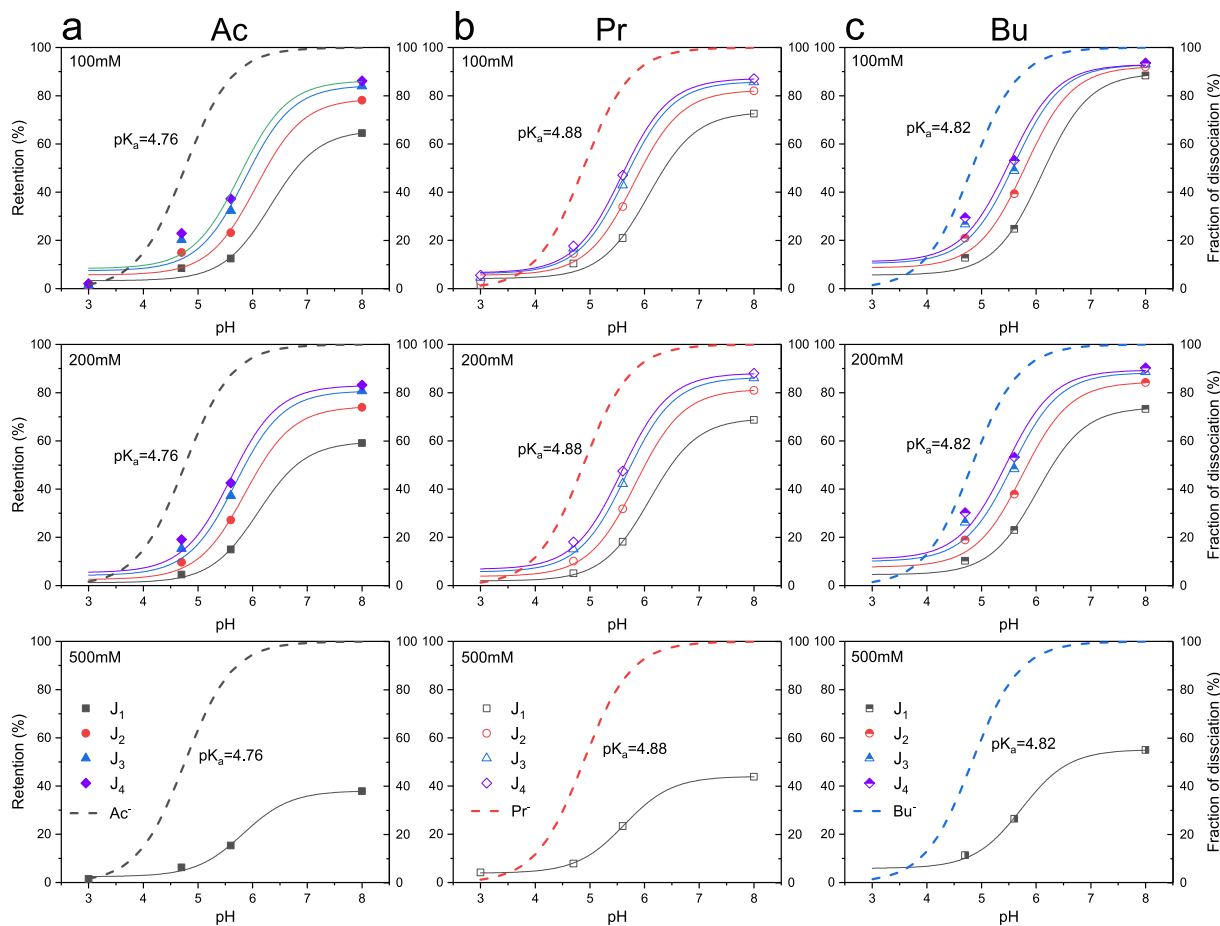


Fig. 2. Retentions of VFAs single solutions at given filtration flux versus solution pH for three concentrations, (a) Ac, (b) Pr, (c) Bu. $J_1 = 0.2 \times 10^{-5} \text{ m s}^{-1}$, $J_2 = 0.5 \times 10^{-6} \text{ m s}^{-1}$, $J_3 = 1 \times 10^{-5} \text{ m s}^{-1}$, $J_4 = 1.5 \times 10^{-5} \text{ m s}^{-1}$, for 500 mM, only J_1 is in the experimental range. The fitting curves are obtained from sigmoid curve fitting by Origin software. The dissociation curves of Ac, Pr, and Bu are given as references, and the pK_a of each VFA is marked in the figure.

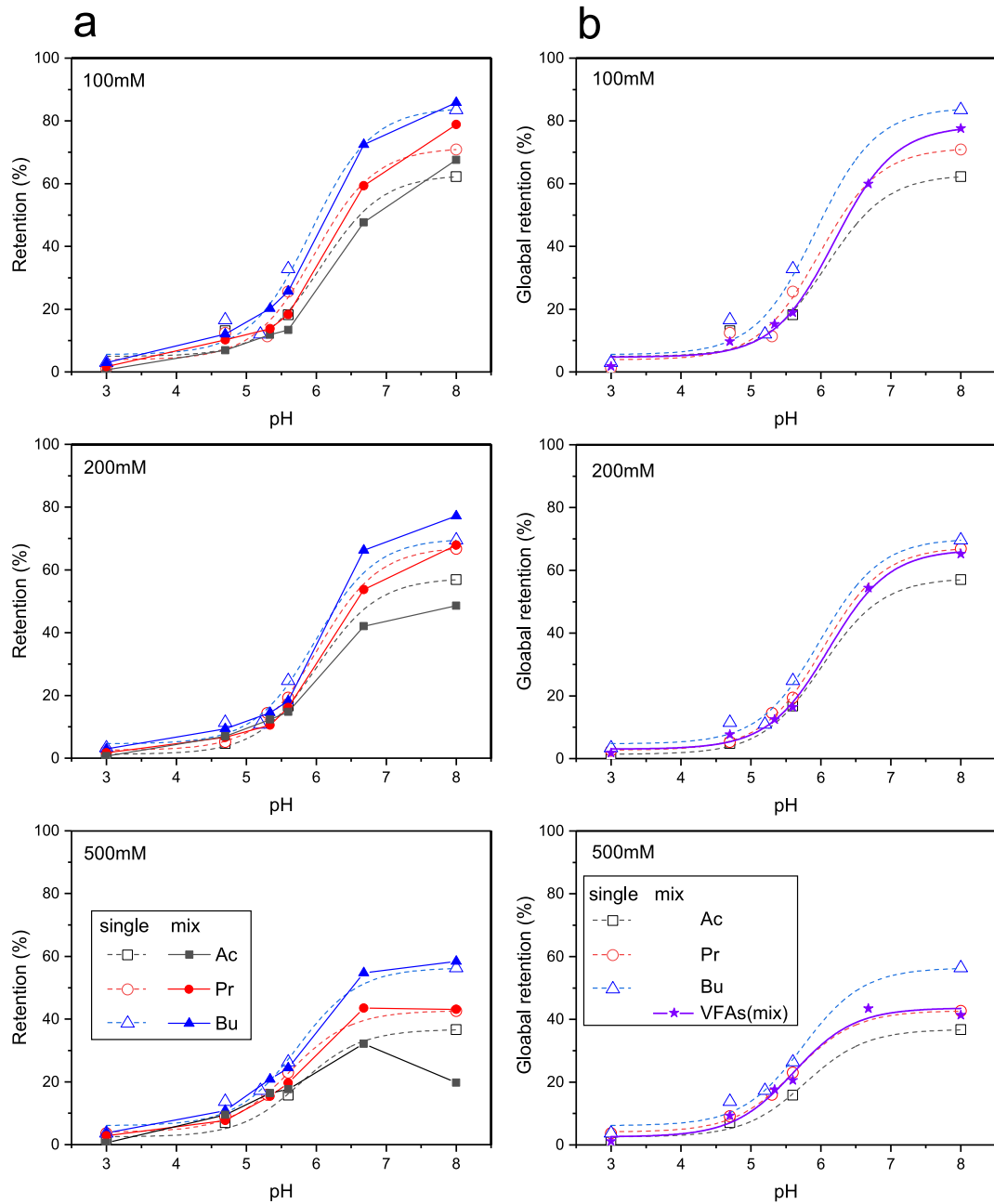


Fig. 3. (a) Individual VFAs retentions, and (b) global retentions of VFAs in Ac/Pr/Bu ternary mixture versus solution pH at three total concentrations and a filtration flux of $2 \times 10^{-6} \text{ m s}^{-1}$.

existence of other VFAs does not influence the individual VFAs retentions in the mixed solutions. Then, similar retentions are expected for single and mixed solutions, as observed. When the pH increases, the contribution of the charge effect gradually increases due to both the increase of the percentage of dissociated VFAs in the solution and the increase of membrane charge. At high pH values, VFAs are dissociated, and the retention of VFAs is dominated by charge effect. Moreover, when two ions with the same charge (co-ions) exist in one solution, charge interaction such as co-ions competition could appear. Indeed, for any electrolyte solution, the electrokinetic charge density is zero (electroneutrality). Therefore, in a system with one counter-ion and two co-ions with different mobilities, greater mobility co-ions are electrostatically attracted to the membrane phase to compensate for the potential deviations from electric neutrality caused by the strong exclusion of the lower mobility co-ions. Thus, a decrease of the retention of the greater

mobility co-ions is observed. Such a phenomenon is generally observed for mixed solutions with less and more retained ions using charged and uncharged membranes [41]. That makes the retention difference between the two individual co-ions bigger than that in their single solutions, as already discussed in previous studies [23,41,42]. For mixed solutions, global VFAs retention is considered for comparison with single solutions.

The weighted average of the individual VFAs retentions in the mixed solutions (namely, global retention, obtained from Eq. (7)) is plotted versus pH for different total concentrations in Fig. 3b. One can observe that the global retention of VFAs increases with pH, following the same trend as that observed for single solutions. Moreover, global retentions are within the individual VFAs retentions in single solutions, i.e., higher than the retention of Ac and lower than the retention of Bu, for all the pH values investigated. Similar trends are observed for the binary solutions

of Ac/Pr and Ac/Bu (results not shown).

3.2. Description of the VFAs retention versus pH

3.2.1. Single solutions

As previously mentioned, the calculation of the VFA retention using Eq. (13) requires knowing the variation of the retention $R_{VFAS^-}(c_{VFAS^-})$ versus the concentration. As an example, Fig. 4 gives the retentions of VFAs in single solutions at a filtration flux of $2 \times 10^{-6} \text{ m s}^{-1}$ and pH 8 versus the concentration. These variations are fitted using Origin® with an exponential function. The functions and the parameters obtained from the fitting for the different solutions are listed in Table 4. For the other filtration flux (J_2 , J_3 , and J_4), the results are not shown.

With the function of $R_{VFAS^-}(c_{VFAS^-})$ provided from Table 4, retentions of VFAs are calculated according to Eq. (13). Fig. 5a gives the variations of the calculated (Eq. (13)) and experimental VFAs retentions in single solutions versus the pH for a given filtration flux J_1 ($2 \times 10^{-6} \text{ m s}^{-1}$) for the three total concentrations investigated. As previously mentioned, both experimental and calculated VFAs retentions increase with solution pH following a sigmoid curve. However, the calculated retentions are always higher than the experimental ones for the three concentrations. The highest differences between calculated and experimental VFAs retentions are observed at the lowest concentration of 100 mM for all the solutions investigated.

Since the size effect is almost not influenced by the pH, this overestimation of retention can be attributed to an overestimation of the charge effect on the VFAs retention. This is confirmed by the more significant overestimation observed at low concentrations.

As previously explained, the charge effect is due to both the solute and membrane charge, which vary with the solution pH according to their respective pK_a values.

The previous calculation was made considering the theoretical pK_a values of the VFAs. Then, Equation (13) was further used to determine the solute pK_{a-f} values, to fit experimental and calculated VFAs retention versus pH variations, using Origin® software. The values of P_{VFAS^-} were obtained from Eq. (10).

The results are reported in Table 5, which gives the fitted pK_{a-f} values and the fitting coefficient of determination (R^2). For comparison, the theoretical pK_a values and the differences between pK_{a-f} and pK_a ($pK_{a-f} - pK_a$) are also given for all the compositions investigated.

One can observe that for each condition, a good fitting is obtained

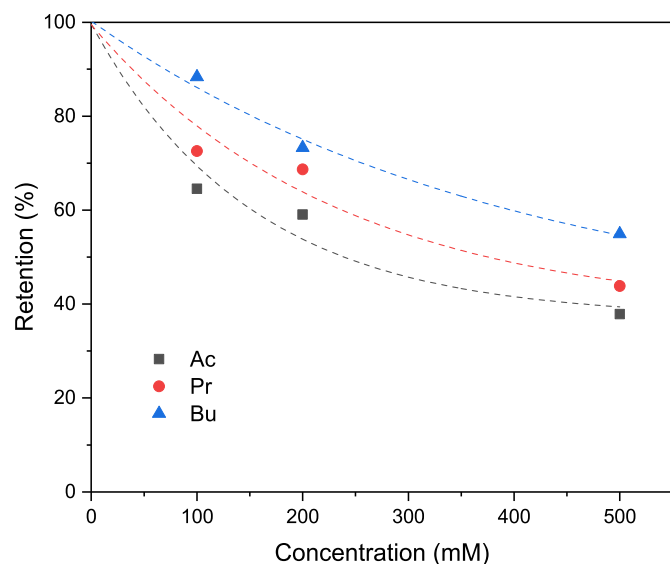


Fig. 4. Retentions of Ac, Pr, and Bu versus concentration at a filtration flux of $2 \times 10^{-6} \text{ m s}^{-1}$ and pH 8. Points are experimental values, and the curves are those from equations in Table 4.

Table 4

VFA retention as a function of ionic concentration at a filtration flux of $2 \times 10^{-6} \text{ m.s}^{-1}$ and pH 8.

Equation	$R_{VFAS^-}(c_{VFAS^-}) = a + b \times c^{c_{VFAS^-}}$		
Parameters	Ac	Pr	Bu
a	0.369	0.368	0.375
b	-0.619	-0.616	-0.631
c	0.00157	0.0168	0.0734
R^2	0.973	0.967	0.993

($R^2 > 0.982$). Then the fitted pK_{a-f} values obtained at different concentrations and proportions are similar; no clear trend is observed. The average pK_{a-f} value for all the compositions is about 1.24 ± 0.09 units higher than the theoretical pK_a values.

Fig. 5b gives the variations of calculated and experimental VFAs retentions versus pH at different concentrations for a given filtration flux J_1 ($0.2 \times 10^{-5} \text{ m s}^{-1}$). Calculated values are obtained from Eq. (13), considering the individual pK_{a-f} values for each solute ($pK_{a-f} = pK_a + 1.24$). It is shown that it is possible to describe the influence of the pH on the VFAs retention using the previous model on condition to consider a modified value of the solutes pK_a that is 1.24 pH units higher than the theoretical values.

The same calculations are made for higher filtration flux (i.e., J_2 , J_3 , and J_4), and the results are given in Table 6. One can observe that for a given solute, the fitted pK_{a-f} decreases when the filtration flux increases. Nevertheless, it remains higher than the theoretical value for the highest filtration flux investigated.

The present results are in agreement with previous ones reporting the variation of the retention of sulfuric acid observed with various NF membranes [32,43]. In these two studies, it was reported that the retention of sulfuric acid starts to increase with solution pH once the pH reaches a value about 1 pH unit higher than its pK_{a2} (1.99). It means that, as concluded in the present work, the variation of retention versus pH could be well fitted considering a pK_a value one unit higher than the theoretical one.

Theoretical pK_a values considered are the ones in the water, at 25 °C and infinite dilution. However, it is known that the properties of the bulk solution can significantly influence the pK_a values of weak acids. For instance, it was reported that the pK_a of acetic acid increases from 4.76 to 9.72 when the dielectric constant of the solvent decreases from $\epsilon = 78.3$ (water, 25 °C) to $\epsilon = 32.64$ (methanol, 25 °C) and that pK_a values of propionic and butyric acids also follow the same trend [44]. Moreover, it is known that in a confined space, the dielectric constant can be lower than in bulk [45]. Then one can expect a higher solute pK_a for a confined solution due to the decrease of the dielectric constant. This phenomenon could be an explanation of the higher pK_a values necessary to fit the results.

On the other hand, calculated values of VFA retentions presented in Fig. 5 were obtained considering that the membrane charge remains constant. Indeed, it was assumed that the retention of the charged VFA was identical to that obtained at pH 8 at the corresponding ionic concentration. However, the proportion of charged solute and the membrane charge can vary with the pH.

In order to consider the variation of the membrane charge with the pH, and its impact on the retention of dissociated VFAs, a correction parameter, α , is introduced in the model. The modified equation is then Eq. (14).

$$R_{VFAS}^{cal} = R_{HVFAS} \times (1 - P_{VFAS^- - pK_a}) + \alpha \times R_{VFAS^-}(c_{VFAS^- - pK_a}) \times P_{VFAS^- - pK_a} \quad (14)$$

$P_{VFAS^- - pK_a}$ is the proportion of dissociated VFAs, $c_{VFAS^- - pK_a}$ is the concentration of dissociated VFAs, calculated with the theoretical pK_a value of the solution.

The correction parameter is obtained by fitting the retention values calculated using Eq. (14) with the experimental ones.

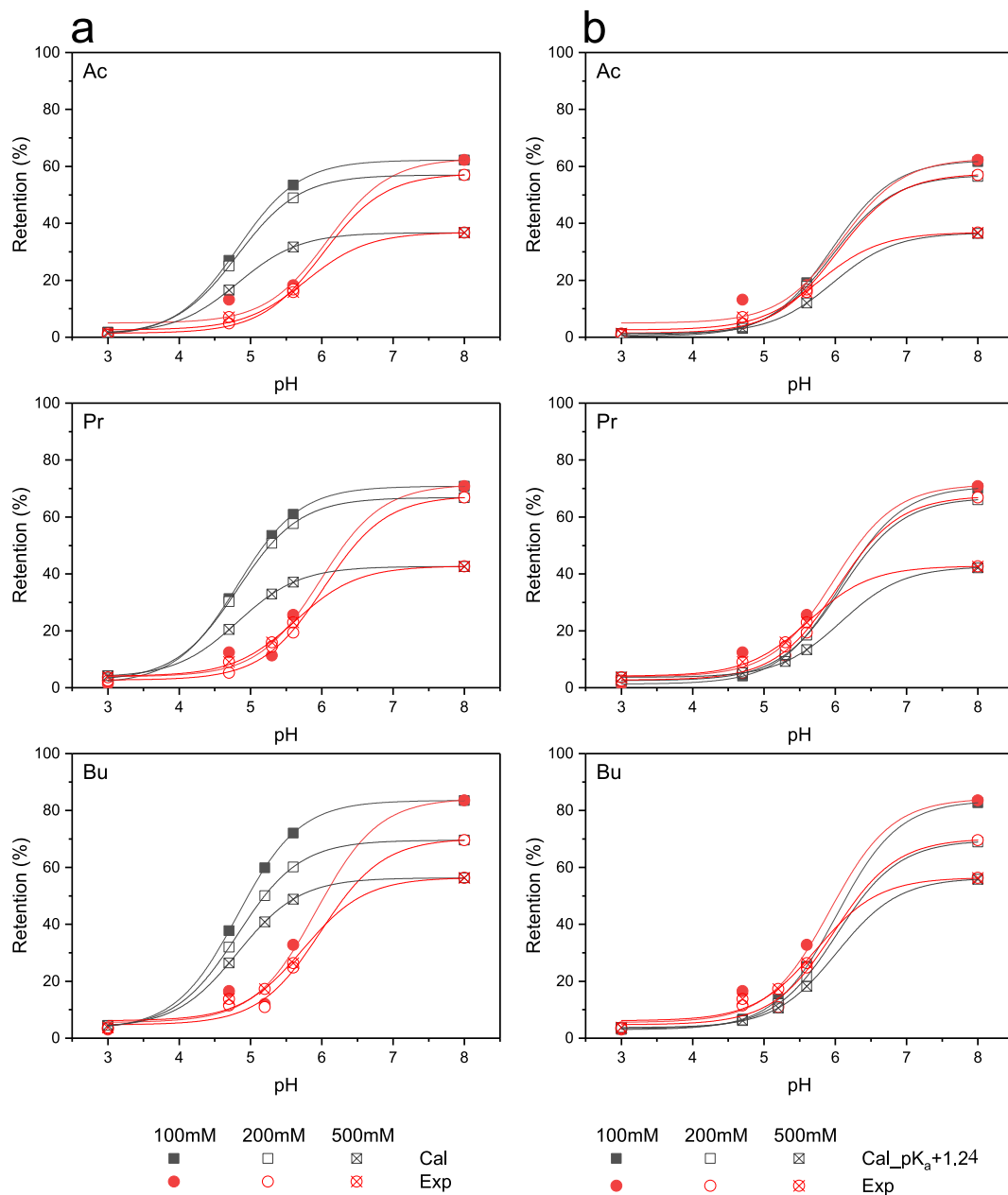


Fig. 5. Calculated and experimental VFAs retention in single solutions versus the solution pH for various total concentrations, filtration flux = $2 \times 10^{-6} \text{ m s}^{-1}$. (a) Calculation using the theoretical pK_a values of VFAs, (b) calculation using the fitted pK_a values that are 1.24 units higher than the theoretical ones ($\text{pK}_{a-f} = \text{pK}_a + 1.24$).

Table 5

Lists of real VFAs pK_a , fitted pK_a , pK_{a-f} , and the differences between pK_a and pK_{a-f} obtained from the fitting of the retention curves at different compositions.

Solutions	100 mM				200 mM				500 mM			
	pK_{a-f}	R^2	pK_a	$\text{pK}_{a-f}-\text{pK}_a$	pK_{a-f}	R^2	pK_a	$\text{pK}_{a-f}-\text{pK}_a$	pK_{a-f}	R^2	pK_a	$\text{pK}_{a-f}-\text{pK}_a$
Ac	6.12	0.983	4.76	1.36	6.11	0.996	4.76	1.35	6.05	0.997	4.76	1.29
Pr	6.07	0.989	4.88	1.19	6.19	0.999	4.88	1.31	6.04	0.999	4.88	1.16
Bu	5.94	0.982	4.82	1.12	6.09	0.995	4.82	1.27	5.92	0.995	4.82	1.10

Following the definition, the correction parameter is equal to 0 at pH 3 and equal to 1 at pH 8. This parameter represents the charge interaction between the solute and the membrane. Since the dissociation of solutes is already taken into account, the value of α is linked to the membrane charge.

The values of α for the three VFAs single solutions at different con-

centrations are plotted versus pH in Fig. 6. One can observe that for each condition α increases with the solution pH following a sigmoid curve. The values obtained for the different solutes at a given concentration are comparable. The values obtained at 100 mM and 200 mM are nearly equal, while those obtained at the highest concentration (500 mM) are higher than low concentrations.

Table 6

Lists of theoretical pK_a , fitted pK_a , pK_{a-f} , and the differences between pK_a and pK_{a-f} obtained from the fitting of the retention curves for single solutions at two concentrations and filtration flux of J_2 ($0.5 \times 10^{-5} \text{ m s}^{-1}$), J_3 ($1 \times 10^{-5} \text{ m s}^{-1}$), and J_4 ($1.5 \times 10^{-5} \text{ m s}^{-1}$).

Solutions	100 mM							200 mM						
	pK_{a-f}			pK_a	$pK_{a-f}-pK_a$			pK_{a-f}			pK_a	$pK_{a-f}-pK_a$		
	J_2	J_3	J_4		J_2	J_3	J_4	J_2	J_3	J_4		J_2	J_3	J_4
Ac	6.06	5.87	5.77	4.76	1.30	1.11	1.01	5.88	5.71	5.61	4.76	1.12	0.95	0.85
Pr	5.81	5.65	5.58	4.88	0.93	0.77	0.70	5.88	5.71	5.63	4.88	1.00	0.83	0.75
Bu	5.82	5.60	5.49	4.82	1.00	0.78	0.67	5.83	5.61	5.49	4.82	1.01	0.79	0.67

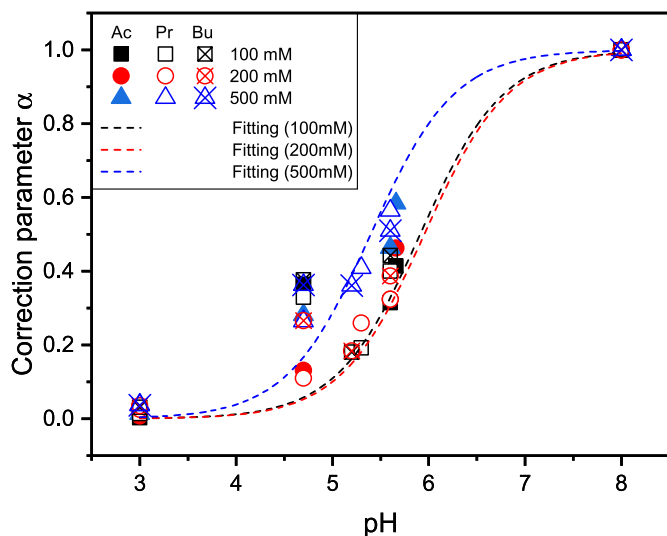


Fig. 6. Correction parameter α (obtained from Eq. (14)) as a function of solution pH at filtration flux $= 0.2 \times 10^{-5} \text{ m s}^{-1}$. Fitting curves (dashed lines) are obtained using Eq. (15) with the pK_{eff} values reported in Table 7.

Considering a pK_{eff} value which representing the effective pK_a of membrane functional groups, the following equation can be written:

$$\alpha = \frac{10^{pH-pK_{eff}}}{1 + 10^{pH-pK_{eff}}} \quad (15)$$

The experimental variations of α versus pH are then fitted using Eq. (15). The corresponding values of pK_{eff} are reported in Table 7. The fitted curves are plotted in Fig. 6.

One can notice that the values are correctly fitted for pH higher than 5.6. For the lower pH, Eq. (15) underestimates the value of α obtained from experimental retentions by Eq. (14).

As previously observed with the α values determined from experimental retentions (Eq. (14)), the pK_{eff} values obtained for different solutions at low concentrations (100 mM and 200 mM) are comparable (5.77 ± 0.02 , and 5.78 ± 0.06 respectively). In contrast, the pK_{eff} values obtained at the highest concentration (500 mM) are about 0.31 units lower (5.47 ± 0.04).

Since pK_{eff} is expected to be related to the pK_a of the membrane functional groups, the values can be compared with those previously

Table 7

Lists of pK_{eff} values (obtained from Eq. (15)) with the coefficient of determination obtained from fitting at different compositions, filtration flux $= 0.2 \times 10^{-5} \text{ m s}^{-1}$.

Solution	100 mM		200 mM		500 mM	
	pK_{eff}	R^2	pK_{eff}	R^2	pK_{eff}	R^2
Ac	5.79	0.822	5.80	0.984	5.52	0.944
Pr	5.74	0.877	5.84	0.990	5.42	0.970
Bu	5.78	0.924	5.69	0.829	5.46	0.892

reported. Indeed, for carboxylic functional groups on polyamide films, pK_a values from 5 to 9 were obtained by contact angle titration [15]. Furthermore, the first pK_a values reported for five different NF/RO membranes with polyamide active layer using heavy ions probes were between 5.23 and 5.72 [9,11]. As a result, one can conclude that pK_{eff} values (from 5.47 to 5.78) obtained in this work are within the range of the membrane pK_a values reported in previous studies.

It was also reported in previous work that the experimental dissociation curves were broadened compared with simulated ones [15]. Current results also show the broadening of the correction parameters versus solution pH compared with simulated dissociation curves (see Fig. 6). This observation could be because carboxylic functional groups on the NF membrane can have different pK_a values, as suggested in previous studies [9,15]. These different pK_a values could be due to the site-site interactions between the functional groups on the polymer chains, which may be related to the low dielectric constant within the aliphatic chain and/or inside the confined membrane pores [9,46,47].

Finally, the two different pK_{eff} values (5.5 for 500 mM and 5.8 for 100 mM and 200 mM) obtained for high and low concentrations indicate that the membrane/solute charge interaction is concentration-dependent. This phenomenon could be due to the ionization of functional groups. Indeed, as previously mentioned concerning VFAs, the ionization constant of a weak acid decreases with ionic concentration according to Debye-Hückel law [48] so that a lower pK_a value can be observed at a higher ionic concentration. The current result is in agreement with this trend.

For membranes with sulfonate groups, the influence of pH on the membrane charge is negligible since sulfonic acid is a strong acid [49]. In a previous study using such a membrane, i.e. NTR-7450 NF, to treat glutathione and three amino acids, it was observed that the retention of charged species of glutathione and L-glutamate increases with the pH and follow the dissociation curve, but with a gap of about 0.5 pH unit [50]. This could suggest that besides the membrane charge, there is an additional influence, like that of the dielectric constant discussed in the present work.

3.2.2. Mixed solutions

The same approach as that used for the single solution can be made for mixed solutions by considering the global retention of the mixed solutions (i.e., the weighted average of the retentions of all the individual VFAs in the mixed solutions, defined in Eq. (7)) and an average solution pK_{a-mix} (calculated from Eq. (12)).

The global retentions of VFAs in mixed solutions at a filtration flux of $2 \times 10^{-6} \text{ m s}^{-1}$ and pH 8 versus the total concentration are given in Fig. 7. The same method is used to fit these variations as that for single solutions. Table 8 listed the functions and the parameters obtained from the fitting for the different solutions.

With the function of $R_{VFAS}(C_{VFAS})$ provided in Table 8, global retentions of VFAs in the mixed solutions at given pH can be calculated according to Eq. (13). The variations of the calculated (Eq. (13)) and experimental global retentions of VFAs in mixed solutions versus the pH for a given filtration flux J_1 ($2 \times 10^{-6} \text{ m s}^{-1}$) for the three total concentrations investigated are presented in Fig. 8a. As observed for single solutions, the retention increases with solution pH following the

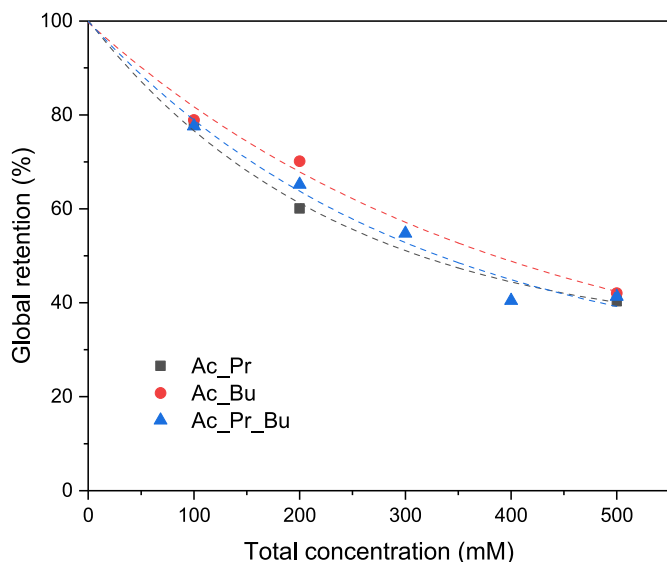


Fig. 7. Global retentions of mixed VFAs solutions (Ac/Pr, Ac/Bu, and Ac/Pr/Bu) versus the total concentration at a filtration flux of $2 \times 10^{-6} \text{ m s}^{-1}$ and pH 8. Points are experimental values, and the curves are those from equations in Table 8.

Table 8

Global retentions of VFAs as a function of ionic concentration at a filtration flux of $2 \times 10^{-6} \text{ m s}^{-1}$ and pH 8.

Equation	$R_{VFAs^-} (C_{VFAs^-}) = a + b \times e^{cVFAs^-}$		
Parameters	Ac/Pr	Ac/Bu	Ac/Pr/Bu
a	0.319	0.188	0.243
b	-0.684	-0.803	-0.754
c	0.0143	0.0863	0.0390
R^2	0.998	0.992	0.988

dissociation curve, and the experimental values are lower than the calculated ones.

The pK_a values, pK_{a-f} , to fit the experimental and calculated variations of the VFAs retention versus pH were determined by Equation (13). Then, the pK_{a-f} values obtained are listed in Table 9, and the difference between pK_{a-f} (fitted pK_a) and theoretical average pK_a of the three solutions (calculated via Eq. (12)) are summarized too. It is observed that the differences between fitted and theoretical ones are 1.24 ± 0.09 , precisely the same as that for single solutions. Then, considering for the solution pK_a values by 1.24 units higher than the theoretical ones, the calculation fits well with the experimental results, as shown in Fig. 8b.

Further calculations for higher filtration flux (i.e., J_2 , J_3 , and J_4) are carried out. The fitted pK_{a-f} values are provided in Table 10. One can observe that, as reported for single VFA solutions, when the filtration flux increases, the fitted pK_{a-f} decreases.

The same as that obtained for single solutions, a correction parameter, α , can be obtained for mixed solutions using Eq. (14). The results are plotted versus pH for the three mixed solutions at different concentrations illustrated in Fig. 9. Then, an effective pK_a value could be used to fit the individual α versus pH. The results are summarized in Table 11.

The pK_{eff} values obtained for different mixed solutions at low concentrations (100 mM and 200 mM) are comparable (5.73 ± 0.13 and 5.82 ± 0.10 , respectively). In contrast, the pK_{eff} values obtained at the highest concentration (500 mM) are about 0.37 units lower (5.40 ± 0.04). Those results are consistent with the results obtained for single solutions (5.77 ± 0.02 for 100 mM, 5.78 ± 0.06 for 200 mM, and 5.47 ± 0.04 for 500 mM). Take all the solutions (single and mixed) into consideration, the pK_{eff} values obtained for VFAs solutions are $5.75 \pm$

0.09 for 100 mM, 5.80 ± 0.08 for 200 mM, and 5.44 ± 0.05 for 500 mM.

To summarize the results obtained with single and mixed solutions at different total concentrations, the average value of the difference between the fitted pK_{a-f} and solution pK_a ($pK_{a-f} - pK_a$) for various compositions (single, binary, and ternary solutions at a total concentration of 100 mM, 200 mM, and 500 mM) is plotted versus filtration flux in Fig. 10. It seems that the influence of total concentration and solution composition is negligible. One can also observe that the difference between pK_{a-f} and pK_a ($pK_{a-f} - pK_a$) decreases for increasing filtration flux, following an exponential curve. As a result, when the filtration flux increases, the pK_{a-f} value approaches the theoretical one. Nevertheless, for the highest filtration flux used in this work, an increase of about 1 unit (1.00 ± 0.24) of the solutes pK_a is still needed to fit the variation of VFAs retention versus pH.

As for single solutions, a pK_{eff} value representing the membrane functional groups was calculated using Eq (15). The corresponding values calculated from the global retentions of VFAs are listed in Table 12. The pK_{eff} values obtained for different solutions are 5.73 ± 0.13 , 5.82 ± 0.10 , and 5.40 ± 0.04 for the total concentrations of 100 mM, 200 mM, and 500 mM, respectively. One can observe that these values are very close to those obtained with single solutions, i.e., 5.75 ± 0.09 , 5.80 ± 0.08 , and 5.44 ± 0.05 , respectively.

Then, one can conclude that in the conditions investigated here, the calculation made with single solutions can be extended to mixed solutions, considering the global retention and an average solution pK_{a-mix} . However, further investigation is still required to check if global retention can still be a suitable parameter for mixtures containing solutes with more different pK_a than those investigated here.

3.3. Conclusion

Solution pH, as well as ionic concentration, have a significant influence on the retention of weak acids, like VFAs, in nanofiltration. Solution pH can change the ratio between the dissociated and undissociated form of weak acids, as well as modify the membrane charge. Ionic concentration can screen the charge interactions between the charged membrane and dissociated weak acids. In this work, the influence of both pH and concentration on the retention of VFAs in single and mixed solutions was investigated.

It was observed that VFAs retention increases with either filtration flux or solution pH. The retention increases with solution pH following the dissociation curves of VFAs. Then, the retention of VFAs decreases when the concentration increases, showing the influence of the screening effect. This influence is negligible at pH 3 and becomes more important when the solution pH increases.

A simple model was proposed to describe the variation of VFA retention versus pH at different concentrations for a given filtration flux.

Only the dissociation of VFAs according to the pH was first considered. It was observed that when using the theoretical solute pK_a values, the calculated retentions were systematically higher than the experimental ones. However, by increasing the pK_a values of the VFAs by up to 1.24 units, the calculated retention curves can fit the experimental ones. It was observed that the pK_a value required to fit the experimental retentions decreases for increasing filtration flux, i.e., it becomes closer to the theoretical value. However, for the highest filtration flux investigated, the difference remains about 1 pH unit. Previous studies have reported that the dielectric constant in a confined space, like membrane pores, is lower than in bulk solution and that pK_a of weak acids like VFA increases when the dielectric constant of the solution decreases. This influence of the dielectric constant could thus explain the highest pK_a values needed to fit the results.

On the other hand, a parameter was introduced to describe the variation of the membrane charge versus pH. This parameter, calculated for each condition to fit the experimental retentions versus pH, was used to determine a membrane pK_{eff} . It was observed that the obtained values, between 5.44 and 5.80, are within the range of the pK_a values

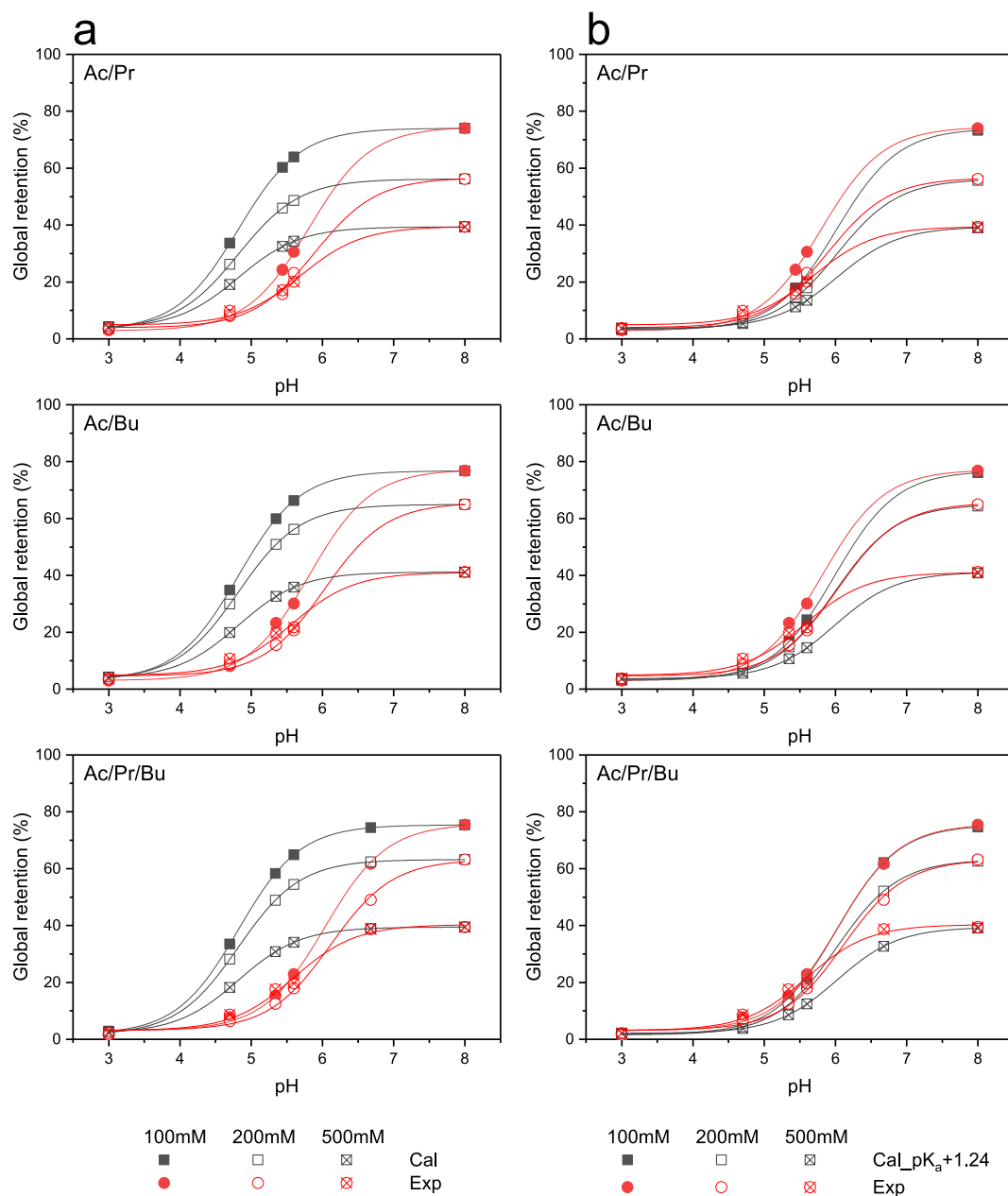


Fig. 8. Calculated and experimental global retentions of VFAs in mixed solutions versus the solution pH for various total concentrations, filtration flux = $2 \times 10^{-6} \text{ m s}^{-1}$. (a) Calculation using the theoretical pK_a values of VFAs, (b) calculation using the fitted pK_a values that are 1.24 units higher than the theoretical ones ($\text{pK}_{a-f} = \text{pK}_a + 1.24$).

Table 9

Lists of theoretical pK_a , fitted pK_a , pK_{a-f} , and the differences between pK_a and pK_{a-f} obtained from the fitting of the retention curves for binary and ternary solutions at three total concentrations at the filtration flux of J_1 ($0.2 \times 10^{-5} \text{ m s}^{-1}$).

Solutions	100 mM				200 mM				500 mM			
	pK_{a-f}	R^2	pK_a	$\text{pK}_{a-f}-\text{pK}_a$	pK_{a-f}	R^2	pK_a	$\text{pK}_{a-f}-\text{pK}_a$	pK_{a-f}	R^2	pK_a	$\text{pK}_{a-f}-\text{pK}_a$
Ac/Pr	5.95	0.999	4.82	1.13	6.14	0.998	4.82	1.32	6.09	0.998	4.82	1.27
Ac/Bu	5.92	0.999	4.79	1.13	6.13	0.998	4.79	1.34	5.93	0.997	4.79	1.14
Ac/Pr/Bu	6.13	0.998	4.82	1.31	6.22	0.998	4.82	1.40	5.95	0.999	4.82	1.13

previously reported for carboxylic functional groups on polyamide films.

Then, it was shown that the methodology developed for single VFA solutions could be used for mixed solutions of VFAs using the global retention and an average solution pK_a . Further work is necessary to determine if this can be applied as well to solutions containing more

different solutes than those investigated here.

Finally, it was not possible to conclude about the best description of the influence of the pH on the membrane/solute interactions, which fix the variation of the retention versus pH. Indeed, both assumptions provided a good description with realistic mechanisms behind: modified

Table 10

Lists of theoretical pK_a , fitted $pK_{a,f}$, $pK_{a,f}$, and the differences between pK_a and $pK_{a,f}$ obtained from the fitting of the retention curves for binary and ternary solutions at two concentrations and filtration flux of J_2 ($0.5 \times 10^{-5} \text{ m s}^{-1}$), J_3 ($1 \times 10^{-5} \text{ m s}^{-1}$), and J_4 ($1.5 \times 10^{-5} \text{ m s}^{-1}$).

Solutions	100 mM							200 mM						
	$pK_{a,f}$			pK_a	$pK_{a,f}-pK_a$			$pK_{a,f}$			pK_a	$pK_{a,f}-pK_a$		
	J_2	J_3	J_4		J_2	J_3	J_4	J_2	J_3	J_4		J_2	J_3	J_4
Ac/Pr	5.82	5.69	5.62	4.82	1.00	0.86	0.80	5.82	5.65	5.56	4.82	1.00	0.83	0.74
Ac/Bu	5.80	5.63	5.55	4.79	1.01	0.84	0.76	5.84	5.63	5.53	4.79	1.05	0.84	0.74
Ac/Pr/Bu	5.90	5.70	5.60	4.82	1.08	0.88	0.78	5.87	5.62	5.47	4.82	1.05	0.80	0.65

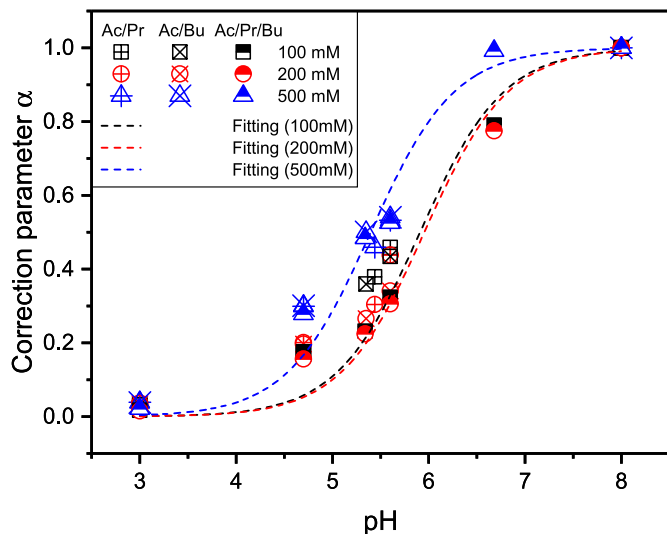


Fig. 9. Correction parameter α (obtained from Eq. (14)) as a function of solution pH at filtration flux $= 0.2 \times 10^{-5} \text{ m s}^{-1}$. Fitting curves (dashed lines) are obtained using Eq. (15) with the pK_{eff} values reported in Table 11.

Table 11

Lists of pK_{eff} values (obtained from Eq. (15)) and the coefficient of determination for the fitting at different compositions, filtration flux $= 0.2 \times 10^{-5} \text{ m s}^{-1}$.

Solution	100 mM		200 mM		500 mM	
	pK_{eff}	R^2	pK_{eff}	R^2	pK_{eff}	R^2
Ac/Pr	5.64	0.987	5.80	0.966	5.36	0.951
Ac/Bu	5.64	0.989	5.71	0.970	5.46	0.946
Ac/Pr/Bu	5.91	0.971	5.95	0.978	5.39	0.970

solution pK_a following confinement on one hand or variation of the membrane charge due to dissociation of functional groups on the other hand. This could be the purpose of further investigation.

Author statement

Yin ZHU: Writing – review & editing. Sylvain Galier: Supervision, Writing – review & editing. H el ene Roux-de Balmann: Supervision, Writing – review & editing

Declaration of competing interest

The authors declare that they have no known competing financial

Nomenclature

List of symbols

J Filtration flux ($\text{m}\cdot\text{s}^{-1}$)

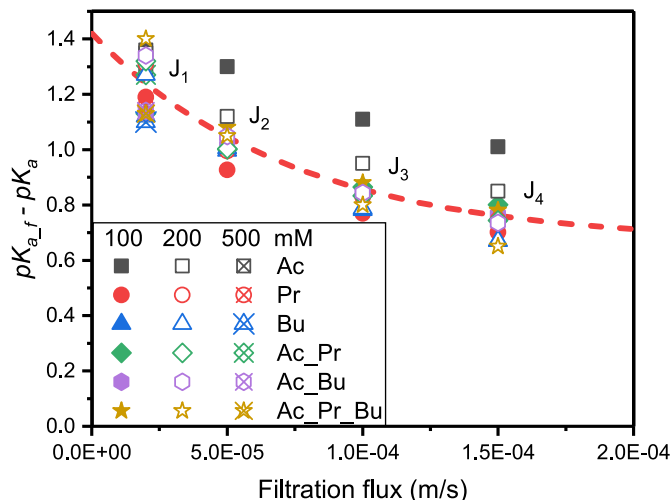


Fig. 10. Average differences between the fitted $pK_{a,f}$ and solution pK_a ($pK_{a,f}-pK_a$) for various compositions (single, binary, and ternary solutions at concentrations of 100 mM, 200 mM, and 500 mM) versus filtration flux.

Table 12

Lists of pK_{eff} values (obtained from Eq. (15)) and the coefficient of determination for the fitting for mixed solutions at different total concentrations, filtration flux $= 0.2 \times 10^{-5} \text{ m s}^{-1}$.

Solution	100 mM		200 mM		500 mM	
	pK_{eff}	R^2	pK_{eff}	R^2	pK_{eff}	R^2
Ac/Pr	5.64	0.987	5.80	0.966	5.36	0.951
Ac/Bu	5.64	0.989	5.71	0.970	5.46	0.946
Ac/Pr/Bu	5.91	0.971	5.95	0.978	5.39	0.970

interests or personal relationships that could have appeared to influence the work reported in this paper.

Acknowledgment

The authors would like to acknowledge the support from Institute Carnot 3BCAR (RECOWER project) and the scholarship provided by the China Scholarship Council (CSC), Ministry of Education, P. R. China for the PhD of Yin ZHU.

<i>V</i>	Volume (m ³)
<i>S_m</i>	Active surface area of the membrane (m ²)
<i>t</i>	Time (s)
<i>R</i>	Retention (%)
<i>C</i>	Concentration (mol·m ⁻³ , abbreviate as mM)
<i>P</i>	Proportion of the solute (%)

Superscripts & subscripts

<i>glo</i>	Global
<i>VFAs</i>	Dissociated and undissociated VFAs
<i>HVFAs</i>	Undissociated VFAs
<i>VFAs⁻</i>	Dissociated VFAs
<i>mix</i>	Mixed solution
<i>sgl</i>	Single solution
<i>Ac</i>	Acetate/acetic acid
<i>Pr</i>	Propionate/propionic acid
<i>Bu</i>	Butyrate/butyric acid
<i>f</i>	Feed
<i>p</i>	Permeate
<i>r</i>	Retentate
<i>exp</i>	Experimental data
<i>cal</i>	Calculated data
<i>m</i>	Membrane

References

- [1] W.S. Lee, A.S.M. Chua, H.K. Yeoh, G.C. Ngoh, A review of the production and applications of waste-derived volatile fatty acids, *Chem. Eng. J.* 235 (2014) 83–99.
- [2] M. Atasoy, I. Owusu-agyeman, E. Plaza, Z. Cetecioglu, Bio-based volatile fatty acid production and recovery from waste streams : current status and future challenges, *Bioresour. Technol.* 268 (2018) 773–786.
- [3] B. Xiong, T.L. Richard, M. Kumar, Integrated acidogenic digestion and carboxylic acid separation by nanofiltration membranes for the lignocellulosic carboxylate platform, *J. Membr. Sci.* 489 (2015) 275–283.
- [4] M.P. Zacharof, S.J. Mandale, P.M. Williams, R.W. Lovitt, Nanofiltration of treated digested agricultural wastewater for recovery of carboxylic acids, *J. Clean. Prod.* 112 (2016) 4749–4761.
- [5] T. Jänisch, S. Reinhardt, U. Pohnsner, S. Böringer, R. Bolduan, J. Steinbrenner, H. Oechsner, Separation of volatile fatty acids from biogas plant hydrolysates, *Separ. Purif. Technol.* 223 (2019) 264–273.
- [6] Y. Yang, C.J. Brigham, C.F. Budde, P. Boccuzzi, L.B. Willis, M.A. Hassan, Z. Abidin, M. Yusof, C. Rha, A.J. Sinskey, Optimization of growth media components for polyhydroxyalkanoate (PHA) production from organic acids by *Ralstonia eutropha*, *Appl. Microbiol. Biotechnol.* (2010) 2037–2045.
- [7] J.M. Gohil, P. Ray, A review on semi-aromatic polyamide TFC membranes prepared by interfacial polymerization: potential for water treatment and desalination, *Separ. Purif. Technol.* 181 (2017) 159–182.
- [8] J. Schaep, C. Vandecasteele, Evaluating the charge of nanofiltration membranes, *J. Membr. Sci.* 188 (2001) 129–136.
- [9] O. Coronell, B.J. Mariñas, X. Zhang, D.G. Cahill, Quantification of functional groups and modeling of their ionization behavior in the active layer of FT30 reverse osmosis membrane, *Environ. Sci. Technol.* 42 (2008) 5260–5266.
- [10] A. Tiraferri, M. Elimelech, Direct quantification of negatively charged functional groups on membrane surfaces, *J. Membr. Sci.* 389 (2012) 499–508.
- [11] O. Coronell, M.I. González, B.J. Mariñas, D.G. Cahill, Ionization behavior, stoichiometry of association, and accessibility of functional groups in the active layers of reverse osmosis and nanofiltration membranes, *Environ. Sci. Technol.* 44 (2010) 6808–6814.
- [12] T. Hoang, G. Stevens, S. Kentish, The effect of feed pH on the performance of a reverse osmosis membrane, *Desalination* 261 (2010) 99–103.
- [13] M. Mänttari, A. Pihlajamäki, M. Nyström, Effect of pH on hydrophilicity and charge and their effect on the filtration efficiency of NF membranes at different pH, *J. Membr. Sci.* 280 (2006) 311–320.
- [14] A. Marecka-Migacz, P.T. Mitkowski, A. Nędzarek, J. Rózański, W. Szaferski, Effect of pH on total volume membrane charge density in the nanofiltration of aqueous solutions of nitrate salts of heavy metals, *Membranes* 10 (2020) 1–20.
- [15] C.C. Wamser, M.I. Gilbert, Detection of surface functional group Asymmetry in interfacially-polymerized films by contact angle titrations, *Langmuir* 8 (1992) 1608–1614.
- [16] A. Bouchoux, H. Roux-de Balman, F. Lutin, Nanofiltration of glucose and sodium lactate solutions: variations of retention between single- and mixed-solute solutions, *J. Membr. Sci.* 258 (2005) 123–132.
- [17] M. Nilsson, G. Trägårdh, K. Östergren, The influence of pH, salt and temperature on nanofiltration performance, *J. Membr. Sci.* 312 (2008) 97–106.
- [18] B. Van Der Bruggen, J. Schaep, D. Wilms, C. Vandecasteele, Influence of molecular size, polarity and charge on the retention of organic molecules by nanofiltration, *J. Membr. Sci.* 156 (1999) 29–41.
- [19] M. Perry, C. Linder, Intermediate reverse osmosis ultrafiltration (RO UF) membranes for concentration and desalting of low molecular weight organic solutes, *Desalination* 71 (1989) 233–245.
- [20] X.L. Wang, A.L. Ying, W.N. Wang, Nanofiltration of L-phenylalanine and L-aspartic acid aqueous solutions, *J. Membr. Sci.* 196 (2002) 59–67.
- [21] A.E. Childress, M. Elimelech, Relating nanofiltration membrane performance to membrane charge (electrokinetic) characteristics, *Environ. Sci. Technol.* 34 (2000) 3710–3716.
- [22] S. Kim, H. Ozaki, J. Kim, Effect of pH on the rejection of inorganic salts and organic compound using nanofiltration membrane, *Kor. J. Chem. Eng.* 23 (2006) 28–33.
- [23] J. Luo, Y. Wan, Effects of pH and salt on nanofiltration—a critical review, *J. Membr. Sci.* 438 (2013) 18–28.
- [24] J. Luo, S. Wei, Y. Su, X. Chen, Y. Wan, Desalination and recovery of iminodiacetic acid (IDA) from its sodium chloride mixtures by nanofiltration, *J. Membr. Sci.* 342 (2009) 35–41.
- [25] Y.H. Weng, H.J. Wei, T.Y. Tsai, W.H. Chen, T.Y. Wei, W.S. Hwang, C.P. Wang, C. P. Huang, Separation of acetic acid from xylose by nanofiltration, *Separ. Purif. Technol.* 67 (2009) 95–102.
- [26] J.-H. Choi, K. Fukushi, K. Yamamoto, A study on the removal of organic acids from wastewaters using nanofiltration membranes, *Separ. Purif. Technol.* 59 (2008) 17–25.
- [27] I.S. Han, M. Cheryan, Nanofiltration of model acetate solutions, *J. Membr. Sci.* 107 (1995) 107–113.
- [28] L.D. Nghiem, A.I. Schafer, M. Elimelech, Role of electrostatic interactions in the retention of pharmaceutically active contaminants by a loose nanofiltration membrane, *J. Membr. Sci.* 286 (2006) 52–59.
- [29] P. Khunnonkwo, K. Jantama, S. Kanchanatawee, S. Galier, H. Roux-de Balman, A two steps membrane process for the recovery of succinic acid from fermentation broth, *Separ. Purif. Technol.* 207 (2018) 451–460.
- [30] J. Schaep, C. Vandecasteele, R. Leysen, W. Doyen, Salt retention of Zirfon (R) membranes, *Separ. Purif. Technol.* 14 (1998) 127–131.
- [31] S. Szoke, G. Patzay, L. Weiser, Characteristics of thin-film nanofiltration membranes at various pH-values, *Desalination* 151 (2002) 123–129.
- [32] J. López, M. Reig, A. Yaroshchuk, E. Licon, O. Gibert, Experimental and theoretical study of nanofiltration of weak electrolytes: SO₄²⁻/HSO₄⁻/H⁺ system, *J. Membr. Sci.* 550 (2018) 389–398.
- [33] M. Reig, O. Gibert, J.L. Cortina, Integration of nano filtration membranes in recovery options of rare earth elements from acidic mine waters, *J. Clean. Prod.* 210 (2019) 1249–1260.
- [34] J.M.K. Timmer, H.C. Vanderhost, T. Robbertsen, Transport of lactic acid through reverse-osmosis and nanofiltration membranes, *J. Membr. Sci.* 85 (1993) 205–216.
- [35] J. López, M. Reig, O. Gibert, J.L. Cortina, Increasing sustainability on the metallurgical industry by integration of membrane nanofiltration processes: acid recovery, *Separ. Purif. Technol.* 226 (2019) 267–277.
- [36] B. Van der Bruggen, J. Schaep, W. Maes, D. Wilms, C. Vandecasteele, Nanofiltration as a treatment method for the removal of pesticides from ground waters, *Desalination* 117 (1998) 139–147.
- [37] P. Somasundaran (Ed.), *Encyclopedia of Surface and Colloid Science*, second ed., CRC Press, New York, 2006.

- [38] B. Balannec, M. Vouch, M. Rabiller-Baudry, B. Chaufer, Comparative study of different nanofiltration and reverse osmosis membranes for dairy effluent treatment by dead-end filtration, *Separ. Purif. Technol.* 42 (2005) 195–200.
- [39] C. Umpuch, S. Galier, S. Kanchanatawee, H. Roux-de Balmann, Nanofiltration as a purification step in production process of organic acids: selectivity improvement by addition of an inorganic salt, *Process Biochem.* 45 (2010) 1763–1768.
- [40] E. Sjoman, M. Manttari, M. Nystrom, H. Koivikko, H. Heikkila, Separation of xylose from glucose by nanofiltration from concentrated monosaccharide solutions, *J. Membr. Sci.* 292 (2007) 106–115.
- [41] Y. Zhu, S. Galier, H.R. de Balmann, Nanofiltration of solutions containing organic and inorganic salts: relationship between feed and permeate proportions, *J. Membr. Sci.* 613 (2020).
- [42] S.H. Kang, Y.K. Chang, Removal of organic acid salts from simulated fermentation broth containing succinate by nanofiltration, *J. Membr. Sci.* 246 (2005) 49–57.
- [43] J. Tanninen, M. Manttari, M. Nystrom, Effect of electrolyte strength on acid separation with NF membranes, *J. Membr. Sci.* 294 (2007) 207–212.
- [44] P. Marshall, E.L.E.E. Purlee, The potentiometric measurement of acid dissociation constants and pH in the system methanol-water. pKa values for carboxylic acids and anilinium ions, *J. Org. Chem.* 20 (1955) 747–762.
- [45] M. Aguilera-arzo, A. Andrio, V.M. Aguilera, A. Alcaraz, Dielectric saturation of water in a membrane protein channel, *Phys. Chem. Chem. Phys.* 11 (2009) 358–365.
- [46] G.J.M. Koper, M. Borkovec, Proton binding by linear, branched, and hyperbranched polyelectrolytes 51 (2010) 5649–5662.
- [47] A. Sadeghpour, A. Vaccaro, S. Rentsch, M. Borkovec, Influence of alkali metal counterions on the charging behavior of poly (acrylic acid), *Polymer* 50 (2009) 3950–3954.
- [48] M. Borkovec, B. Jönsson, G.J.M. Koper, Ionization processes and proton binding in polyprotic Systems : small molecules, proteins, interfaces and polyelectrolytes, in: E. M (Ed.), *Surf. Colloid Sci.*, Springer, Boston, MA, 2001, pp. 99–339.
- [49] C. Zeng, S. Tanaka, Y. Suzuki, S. Fujii, Impact of feed water pH and membrane material on nanofiltration of perfluorohexanoic acid in aqueous solution, *Chemosphere* 183 (2017) 599–604.
- [50] T. Gotoh, H. Iguchi, K.C. Kikuchi, Separation of glutathione and its related amino acids by nanofiltration, *Biochem. Eng. J.* 19 (2004) 165–170.